

Macromolecular Design via an Organocatalytic, Monomer-Specific and Temperature-Dependent “On/Off Switch”. High Precision Synthesis of Polyester/Polycarbonate Multiblock Copolymers

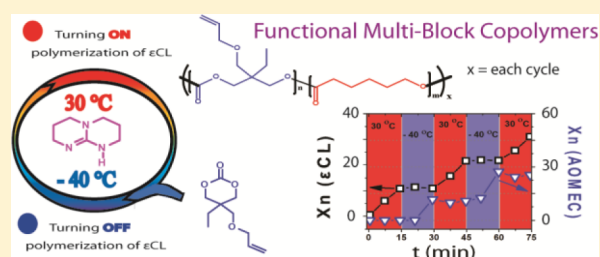
Peter Olsén,[†] Karin Odelius,[†] Helmut Keul,[‡] and Ann-Christine Albertsson^{*,†}

[†]Department of Fibre and Polymer Technology, KTH Royal Institute of Technology, SE-100 44, Stockholm, Sweden

[‡]DWI – Leibniz Institute for Interactive Materials and Institute of Technical and Macromolecular Chemistry, RWTH Aachen University, Forckenbeckstraße 50, D-52056 Aachen, Germany

S Supporting Information

ABSTRACT: The employment of a monomer-specific “on/off switch” was used to synthesize a nine-block copolymer with a predetermined molecular weight and narrow distribution ($\mathcal{D} = 1.26$) in only 2.5 h. The monomers consisted of a six-membered cyclic carbonate (i.e., 2-allyloxymethyl-2-ethyl-trimethylene carbonate (AOMECA)) and ϵ -caprolactone (ϵ CL), which were catalyzed by 1,5,7-triazabicyclo[4.4.0]-dec-5-ene (TBD). The dependence of polymerization rate with temperature was different for the two monomers. Under similar reaction conditions, the ratio of the apparent rate constant of AOMECA and ϵ CL [$k_p^{\text{app}}(\text{AOMECA})/k_p^{\text{app}}(\epsilon\text{CL})$] changes from 400 at $T = -40\text{ }^\circ\text{C}$ to 50 at $T = 30\text{ }^\circ\text{C}$ and 10 at $T = 100\text{ }^\circ\text{C}$. Therefore, by decreasing the copolymerization temperature from $30\text{ }^\circ\text{C}$ to $-40\text{ }^\circ\text{C}$, the conversion of ϵ CL can be switched “off”, and by increasing the temperature to $30\text{ }^\circ\text{C}$, the conversion of ϵ CL can be switched “on” again. The addition of AOMECA at $T = -40\text{ }^\circ\text{C}$ results in the formation of a pure carbonate block. The cyclic addition of AOMECA to a solution of ϵ CL along with a simultaneous temperature change leads to the formation of multiblock copolymers. This result provides a new straightforward synthetic route to degradable multiblock copolymers, yielding new interesting materials with endless structural possibilities.



INTRODUCTION

Nature’s ability to produce materials with exact structures on all levels of order continues to allure and inspire every generation of polymer chemist. It is safe to say that, to date, the scientific community does not measure up to nature’s synthetic machinery. Although, considerable efforts are made enlarging and refining the macromolecular tool-box within the vision of macromolecular design perfection.^{1–4} From a polymer synthetic point of view, many of nature’s polymers can be described as multiblock copolymers, where each block is constituted of one or more repeating unit. However, synthetic control for one unit additions is very demanding, but in principle, similar polymeric behavior should be reachable by a block approach. This has given rise to an ever increasing interest for multiblock copolymers within the field of polymer science. Most activity regarding this issue has been seen in the field of controlled radical polymerization, since it enables the creation of multiblocks by sequential addition scheme.^{5,6} However, regarding ring-opening polymerization of aliphatic polyesters, the same rules does not apply, and high conversion is always accompanied by an increased probability for transesterification reactions that reshuffles the polymer sequence.

On the other hand ring-opening polymerization of cyclic monomers enables the formation of a variety of polymers with

different functionality and properties with major applications in the field of polymer technology. Traditionally, the catalytic ring-opening polymerization of lactones and cyclic carbonates was usually performed with metallic catalysts, such as lithium, sodium and potassium alkoxides, aluminum alkoxides, tin(IV) alkoxides, and tin(II) carboxylates, in combination with alcohols. The obtained polyesters and polycarbonates are degradable and have a large potential for application as biomaterials. However, the degradability is often influenced by the residual metallic catalyst. Currently, organocatalysts have been developed that are used along with alcohols as initiators for the ring-opening polymerization of lactones and cyclic carbonates. The employed catalytic system directly dictates the rate of polymerization and control over the molecular weight and dispersity as well as the structure and architecture of the final polymer, enabling the preparation of tailor-made polymers for specific applications.^{7–10}

Macromolecular design of polymers and copolymers adds an additional layer of complexity that further facilitates control over material properties, which have been realized in the synthesis of star-shaped^{11,12} and branched^{13,14} as well as,

Received: February 5, 2015

Revised: February 27, 2015

Published: March 6, 2015

statistical, tapered,^{15–17} and block copolymers.^{18–21} The traditional approach for the synthesis of specific di-, tri-, or multiblock copolymers includes sequential addition of monomers to the initiator or coupling of reactive building blocks. However, both procedures are synthetically plagued by drawbacks, such as the sequential addition requiring a high conversion of the antecedent monomer and coupling reactions typically exhibit high dispersity and large amounts of unconverted building blocks.^{22–25} However, if the monomer polymerizability is altered via an external stimulus during polymerization, it should be possible to overcome these shortcomings.

Organocatalyzed ring-opening polymerization has experienced an upsurge of activity since the initial reports on the polymerization of lactide with 4-dimethylaminopyridine (DMAP).^{26,27} Today, numerous organocatalytic systems have been explored that exhibit an array of different specificities toward selected monomers.^{28–32} In particular, the difference in reactivity of cyclic carbonates and cyclic esters (lactones) has been observed where the polymerization is catalyzed by semiweak acids, which exhibit a higher reactivity for esters,^{32–35} in contrast to guanine adenine base-catalyzed systems.^{34–37} Recently, this result has been pushed to the limit by sequentially “switching” from an anionic to a cationic organocatalyzed system, enabling specific monomer selectivity.^{38,39}

Over the years, we have worked extensively in the field of degradable polymers, and most of these polymers have been prepared by ring-opening polymerization of lactones, lactides, and other functional monomers,^{40–43} with great emphasis on a “cradle to grave” perspective, from the kinetics of polymer formation to the kinetics of polymer degradation.^{44–46} In addition, we explored the synthesis of aliphatic carbonate monomers via ring-closing depolymerization and its polymerization behavior with different catalysts.^{47–49}

Therefore, we envision that the difference in selectivity between cyclic esters and cyclic carbonates induced by organic catalysts should engender control, enabling the formation of functional multiblock copolymers in a simultaneous addition scheme. Our aim is to elaborate this conceptually, the creation of multiblock copolymers through a monomer specific “on/off switch”. To elucidate this approach, we focused our exploration around three different queries as follows: (i) how is the macromolecular structure (i.e., block purity) affected by the organic catalyst employed, (ii) how is this effect dependent on temperature, and (iii) how does this translate into multiblock copolymer design?

EXPERIMENTAL SECTION

Materials. ϵ -Caprolactone (ϵ CL) (98%, Sigma-Aldrich, Sweden) was dried over calcium hydride for at least 24 h and subsequently distilled at reduced pressure under an inert gas atmosphere prior to use. All of the other chemicals were used as received. These chemicals included initiators (i.e., benzyl alcohol ($\geq 99\%$, Sigma-Aldrich, Sweden) and 2-naphthalene ethanol (98%, Sigma-Aldrich, Sweden)), catalysts (i.e., 1,5,7-triazabicyclo[4.4.0]-dec-5-ene (TBD) (98%, Sigma-Aldrich, Sweden)), and a phosphazene base P_2 -*t*Bu solution (P_2 -*t*Bu, ~ 2 M in THF, Sigma-Aldrich, Sweden). In addition, sodium hydride (NaH) (60% dispersion in mineral oil, Sigma-Aldrich, Sweden), diethyl carbonate (99%, Sigma-Aldrich, Sweden), trimethylolpropane allyl ether (98%, Sigma-Aldrich, Sweden), acetic acid (technical, Fisher Scientific, Germany), acetic acid anhydride (ReagentPlus, $\geq 99\%$, Sigma-Aldrich, Sweden), triethylamine (TEA) ($\geq 99\%$, Sigma-Aldrich, Sweden), dichloromethane (anhydrous, \geq

99.8%, Sigma-Aldrich, Sweden) chloroform (HPLC grade, Fisher Scientific, Germany), chloroform-*d* (99.8%, with silver foil, Cambridge Isotope Laboratories), and methanol (general purpose grade, Fischer Scientific, Germany) were used.

Synthesis of AOMECE. The monomer synthesis was performed via ring-closing depolymerization according to a previously reported protocol,⁴⁷ except for a consecutive distillation step with the addition of acetic anhydride (0.1 equiv to AOMECE) and TEA (0.1 equiv to AOMECE) to ensure that any residual hydroxyl groups are capped.

Copolymerization of 2-Allyloxmethyl-2-ethyltrimethylene Carbonate (AOMECE) and ϵ -Caprolactone (ϵ CL). General experimental methodology: All of the reaction vessels were dried in an oven at 150 °C for 48 h prior to use followed by flaming three times under reduced pressure. In general, the desired amounts of monomers, catalyst and initiator were added to a Schlenk round-bottom flask under a nitrogen atmosphere in a glovebox (Mbraun MB 150-GI). After addition, the flask was fitted with a rubber septum and placed in an oil bath outside the glovebox (Mbraun MB 150-GI). All of the reactions were stirred at a constant temperature that was maintained (± 2 °C) using an IKAMAG RCT basic safety control magnetic stirrer. Aliquots for investigation by ¹H NMR and ¹³C NMR spectroscopy as well as GPC were withdrawn at regular time intervals using new, disposable syringes while the vessel was flushed with nitrogen gas. Each sample was treated with acetic acid dissolved in DCM.

Copolymerization of AOMECE and ϵ CL at 30 °C, Catalyzed with TBD. The desired amounts of the monomers (i.e., AOMECE (3 g, 15 mmol) and ϵ CL (1.71 g, 15 mmol)) and the benzyl alcohol initiator (0.016 g, 0.15 mmol) were added to a dried 25 mL Schlenk round-bottom flask inside a glovebox. The copolymerization was performed in a 2 M solution of dry DCM. The TBD (0.053 g, 0.38 mmol) was dissolved in dry DCM (5 mL) inside a glovebox and injected into the reaction mixture via a disposable syringe. All of the copolymerization experiments were performed according to this specific procedure (Table 1).

Table 1. Copolymerization of AOMECE and ϵ CL at Different Temperatures Initiated by Benzyl Alcohol/TBD or P_2 -*t*Bu

temperature [°C]	catalyst	[M] ^a : [1]: [Cat.]	solvent	concn [M]
−40	TBD	[200]: [1]: [2.5]	DCM	2
30	TBD	[200]: [1]: [2.5]	DCM	2
100	TBD	[200]: [1]: [2.5]	none	bulk
170	TBD	[200]: [1]: [2.5]	none	bulk
30	P_2 - <i>t</i> Bu	[400]: [1]: [0.5]	DCM	2

$$^a[M], M = n_{\text{AOMECE}} + n_{\text{\epsilon CL}} \text{ and } n_{\text{AOMECE}}/n_{\text{\epsilon CL}} = 1.$$

TBD-Catalyzed Copolymerization of AOMECE and ϵ CL with Temperature Variation. The polymerization was performed in a similar manner as previously described with some minor modifications. Specifically, the desired amounts of initiator (i.e., 2-naphthalene ethanol (0.051 g, 0.3 mmol)) and catalyst (i.e., TBD (0.62 g, 4.46 mmol)) were added to a 50 mL Schlenk flask inside a glovebox. The reaction flask was placed in a thermostatic oil bath set at 30 °C followed by the addition of 29 mL of dry DCM. After 5 min, ϵ CL (6.84 g, 60 mmol) was added to the reaction mixture with a disposable syringe (1.8 M, where $n = n_{\text{\epsilon CL}} + n_{\text{TBD}} + n_{\text{AOMECE}}$). After 15 min (ϵ CL had reached a conversion of approximately 7%), the temperature was lowered to −40 °C and allowed to equilibrate for 7.5 min. At this temperature, no further conversion of ϵ CL was observed. After the equilibration, AOMECE (2 g, 10 mmol) was added to the reaction mixture using a disposable syringe. After near complete conversion of AOMECE (7.5 min later), the reaction flask was again placed in a thermostatic oil bath at 30 °C, and the same cycle was repeated three consecutive times, resulting in a ϵ CL conversion of 14, 21, 28 and 35%. At each 7.5 min interval, a sample was withdrawn using a disposable syringe, treated with acetic acid dissolved in DCM and analyzed by ¹H and ¹³C NMR spectroscopy as well as GPC. The k_p^{app} values was determined by plotting the $\ln(M_0/M)$ vs time, Supporting Information, Figures S1–S5.

Table 2. Apparent Rate Constant (k_p^{app}) at Different Temperatures for AOMECE and ϵ CL during Copolymerization Initiated by Benzyl Alcohol/TBD or P2-*t*-Bu

temperature [°C]	catalyst	[M] ^a :[I]:[Cat.]	$k_p^{\text{app}}(\text{AOMECE})^b$ [s ⁻¹]	$k_p^{\text{app}}(\epsilon\text{CL})^b$ [s ⁻¹]
-40	TBD	[200]:[1]:[2.5]	25	0.064
30	TBD	[200]:[1]:[2.5]	17.1	0.35
100	TBD	[200]:[1]:[2.5]	630	65.4
170	TBD	[200]:[1]:[2.5]	190	102
30	P2- <i>t</i> -Bu	[400]:[1]:[0.5]	101.9	21.5

^a[M], M = $n_{\text{AOMECE}} + n_{\epsilon\text{CL}}$ and $n_{\text{AOMECE}}/n_{\epsilon\text{CL}} = 1$. ^bFor determination of k_p^{app} values see Supporting Information figure S1–S5.

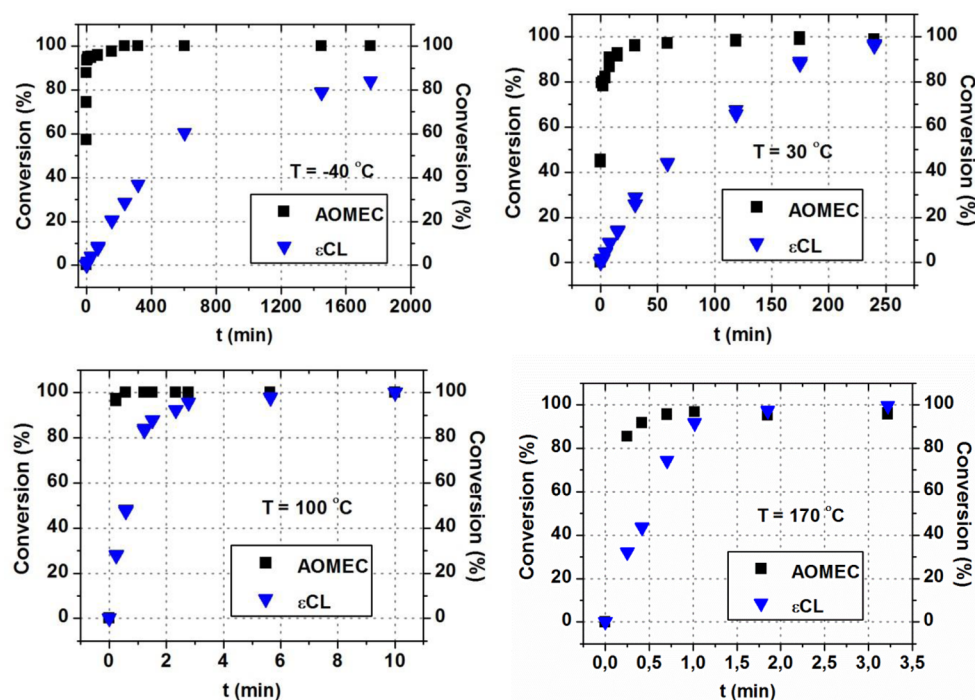


Figure 1. Dependence of the conversion on the time for the copolymerization of AOMECE ($n_{\text{AOMECE}}/n_{\text{Bn-OH}} = 100$) and ϵ CL ($n_{\epsilon\text{CL}}/n_{\text{Bn-OH}} = 100$). Solution polymerizations at -40 (top left) and +30 °C (top right) were performed in dry DCM (2 M to $n_{\text{AOMECE}} + n_{\epsilon\text{CL}}$). At 100 (bottom left) and 170 °C (bottom right), the polymerizations were performed in bulk. All of the polymerizations were conducted with TBD ($n_{\text{TBD}}/n_{\text{Bn-OH}} = 2.5$) as the catalyst.

Instruments. Nuclear Magnetic Resonance (NMR). The ¹H NMR (400.13 MHz) and ¹³C NMR (100.62 MHz) spectra were recorded on a Bruker Avance 400 spectrometer at 298 K. For the measurements, either ~10 mg (¹H NMR) or ~100 mg (¹³C NMR) of the polymer was dissolved in 0.8 mL of CDCl₃ in a sample tube with a diameter of 5 mm. The spectra were calibrated using the residual proton of the solvent signal (i.e., 7.26 ppm (¹H NMR) and 77.0 ppm (¹³C NMR)) for CHCl₃.

Gel Permeation Chromatography (GPC). GPC was used to determine the number-average molecular weights (M_n) and dispersity (D_s) of the polymer using a Verotech PL-GPC 50 Plus equipped with a PL-RI detector and two MIXED-D columns that were 300 × 7.5 mm (Varian, Santa Clara). The samples were injected with a PL-AS RT autosampler (Polymer Laboratories), and chloroform was used as the mobile phase at a flow rate of 1 mL/min at 30 °C with toluene as an internal standard. The calibration was performed using polystyrene standards with a narrow molecular weight distribution ranging from 160–371000 g/mol.

RESULTS AND DISCUSSION

The search for new synthetic methodologies that result in multiblock copolymers with high control of block purity, predictable molecular weight, and narrow distributions has led us to explore the organocatalytic copolymerization of lactones

and cyclic carbonates. More specifically, we studied the copolymerization behavior of AOMECE and ϵ CL as a function of (i) different organocatalysts with different reactivity of the propagating chain end and (ii) different temperatures as well as (iii) the translation of these results into the design of multiblock copolymers.

Influence of the Reactivity of the Propagating Chain Ends and Effect on the Selectivity toward AOMECE and ϵ CL. The reactivity of the two monomers and the propagating chain ends differs substantially with the catalytic system employed, which dictates the monomer sequence in the formed polymeric structure. This difference is especially true in the AOMECE/ ϵ CL system. The polymerization of AOMECE was first explored in the beginning of the 1990s. Herein, it was found that, polymerization under anionic condition results in a bimodal distribution: alongside a fraction of linear high molecular weight polymers cyclic oligomers were also formed. The ratio of linear polymers to cyclic oligomers strongly depends on the reaction conditions, such as monomer concentration, solvent used, temperature and time.^{50,51} However, when TBD was applied as a catalyst for the polymerization of AOMECE, none of these effects were observed, and the only product was a high molecular weight

Scheme 1. Synthetic Outline for the Copolymerization of AOMECE ($n_{\text{AOMECE}}/n_{\text{Bn-OH}} = 100$) and ϵCL ($n_{\epsilon\text{CL}}/n_{\text{Bn-OH}} = 100$) with TBD ($n_{\text{TBD}}/n_{\text{Bn-OH}} = 2.5$) as a Catalyst

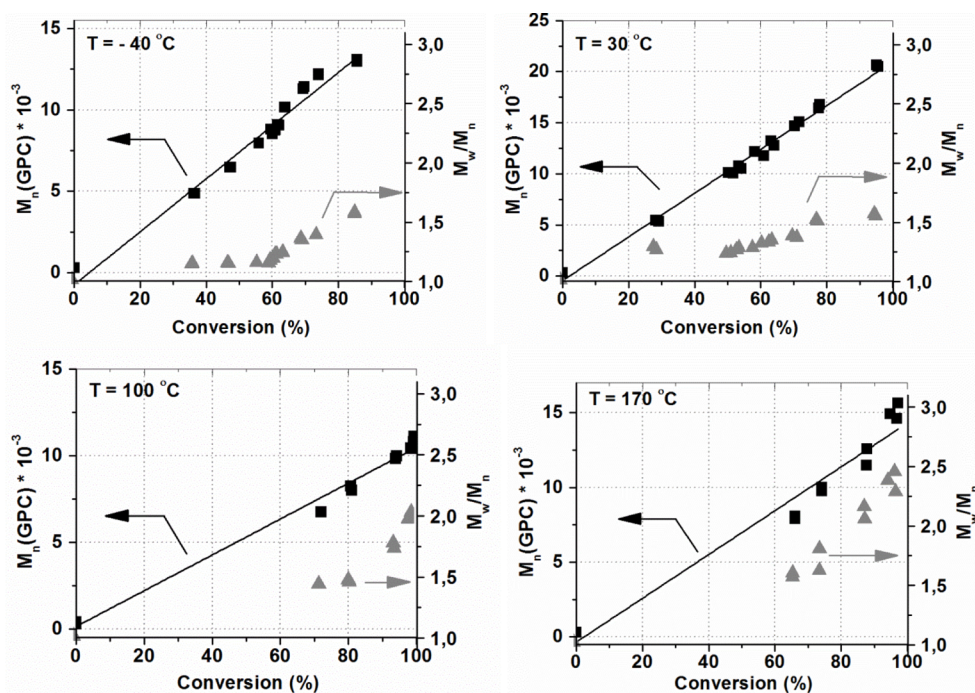
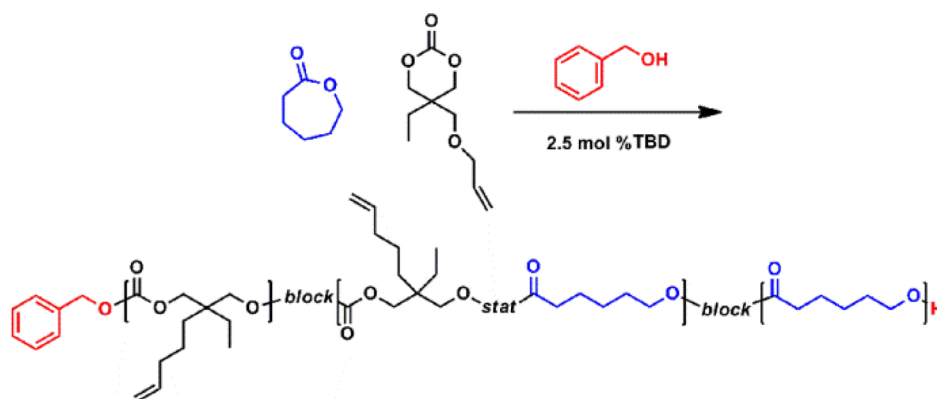


Figure 2. M_n and \bar{D} evolution as a function of conversion for the copolymerization of AOMECE ($n_{\text{AOMECE}}/n_{\text{Bn-OH}} = 100$) and ϵCL ($n_{\epsilon\text{CL}}/n_{\text{Bn-OH}} = 100$). Solution polymerizations at -40 (top left) and $+30$ °C (top right) were performed in dry DCM (2 M to $n_{\text{AOMECE}} + n_{\epsilon\text{CL}}$). At 100 (bottom left) and 170 °C (bottom right), the polymerizations were performed in bulk. All of the polymerizations were conducted using TBD ($n_{\text{TBD}}/n_{\text{Bn-OH}} = 2.5$) as the catalyst.

polymer.⁴⁷ Therefore, to more deeply explore the influence of the nature of the propagating chain end, two different nonmetallic catalysts with different effects on the reactivity of the propagating chain were chosen (i.e., TBD and a phosphazene base, P2-*t*-Bu). Time conversion plots for the copolymerization of AOMECE and ϵCL with benzyl alcohol (Bn-OH) as an initiator and TBD as a catalyst in a methylene chloride solution at $T = 30$ °C clearly indicate that AOMECE polymerizes much faster than ϵCL (Supporting Information, Figure S8, left). The apparent rate constant for AOMECE was ca. 50 times higher than the apparent rate constant for ϵCL (Table 2). The linear relationship between M_n and conversion and the low dispersity confirm the controlled course of the reaction. When the same reaction conditions for the P2-*t*-Bu catalyst, an immeasurably high polymerization rate was observed. Therefore, we reduced the catalyst loading by a factor of 2.5 ($n_{\text{P2-}t\text{-Bu}}/n_{\text{BuOH}} = 1$) to determine the kinetic

parameters. Even at this low catalyst loading, a high rate of polymerization was observed ($k_p^{\text{app}}(\text{AOMECE}) = 101.9 \text{ s}^{-1}$, $k_p^{\text{app}}(\epsilon\text{CL}) = 21.5 \text{ s}^{-1}$, (Table 2, Supporting Information Figures S5 and S9). The rate of polymerization reflects the influence of TBD and P2-*t*-Bu on the reactivity of the propagating chain end during homopolymerization and copolymerization of AOMECE and ϵCL .

Besides the high rate of polymerization the P2-*t*-Bu-catalyzed system produced an oligomeric fraction during polymer formation, which is similar to that previously observed for the anionic polymerization of AOMECE (Supporting Information, Figure S6, S7).⁵⁰ This result is believed to be due to the effect of a higher concentration of solvent separated ion pairs (sip) originating from the ability of the phosphazene base to solvate the active chain end, which leads to a polymerization with more anionic character.⁵² This behavior is also reflected in the immense difference in the polymerization rate between the two

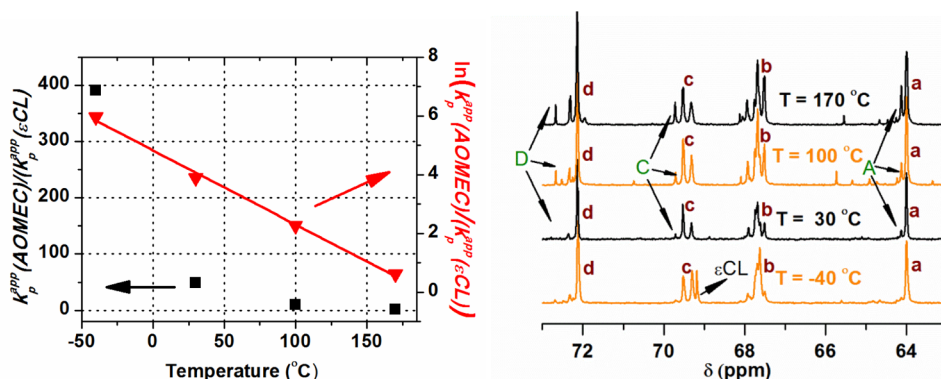
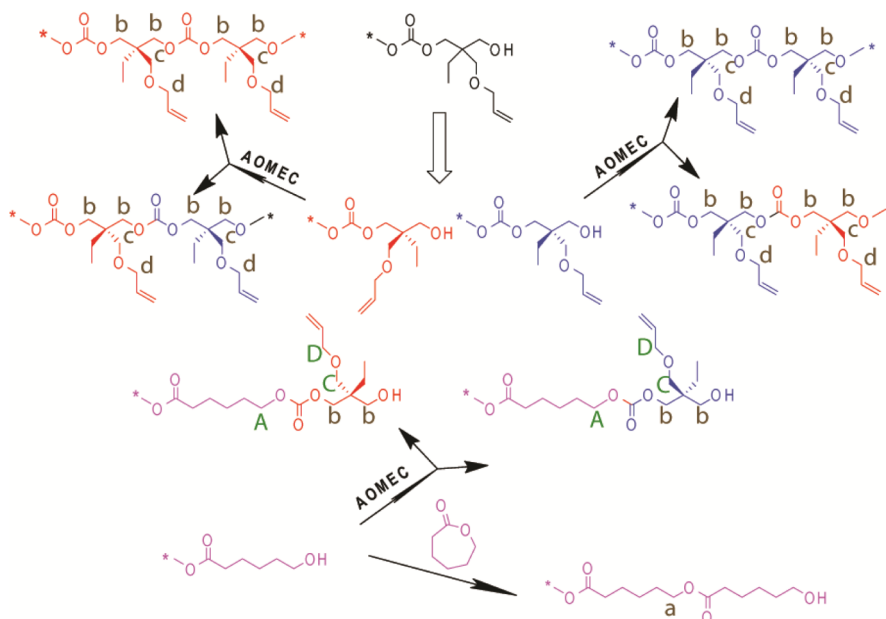


Figure 3. Quotient of the rate constants during the copolymerization of AOMECE ($n_{\text{AOMECE}}/n_{\text{Bn-OH}} = 100$) and ϵCL ($n_{\epsilon\text{CL}}/n_{\text{Bn-OH}} = 100$) with TBD ($n_{\text{TBD}}/n_{\text{Bn-OH}} = 2.5$) as the catalyst (left) and its influence on the block purity shown in the ^{13}C NMR (right). For letter notation, see Scheme 2.

Scheme 2. Outline of the Different Diads Formed during the Copolymerization of AOMECE ($n_{\text{AOMECE}}/n_{\text{Bn-OH}} = 100$) and ϵCL ($n_{\epsilon\text{CL}}/n_{\text{Bn-OH}} = 100$) Using TBD ($n_{\text{TBD}}/n_{\text{Bn-OH}} = 2.5$) as the Catalyst Arising from the Racemic Nature of AOMECE



systems (i.e., ~ 6 times higher for AOMECE and ~ 60 times higher for ϵCL) (Table 2, Supporting Information, Figures S2 and S5). In addition, the high rate of polymerization for the P2-*t*-Bu-catalyzed copolymerization resulted in a higher dispersity (compare Supporting Information, Figures S8 and S9). On the basis of these results, TBD was chosen as the catalyst for the preparation of multiblock copolymers in our new synthetic strategy.

Effect of Temperature on the Copolymerization of AOMECE and ϵCL with TBD as the Catalyst and Its Effect on the Block Structure. In a previous study of the anionic ring-opening copolymerization of 2,2-dimethyl trimethylene carbonate and ϵCL , the carbonate was reported to polymerize much faster.⁵³ The same result was obtained for AOMECE and ϵCL using TBD/benzyl alcohol as the initiating system (Figure 1). However, the temperature dependence of the conversion of the two monomers and its effect on the polymer microstructure (i.e., the monomer selectivity) has not been previously explored. Therefore, the monomer conversions were evaluated as a function of temperature and its effect on the microstructure were qualitatively evaluated (Scheme 1). In addition, the

synthetic prerequisites for the formation of pure block copolymers were determined. It is important to note that the polymer microstructure is not determined solely by the difference in polymerization rate. More specifically, due to the low ceiling temperature ($T_c = 190$ °C), the conversion of AOMECE will reach a plateau that is temperature dependent. Therefore, the block purity will be highly influenced by the equilibrium monomer concentration. In addition, transesterification may lead to reshuffling of the monomer sequence.

The most obvious difference in the copolymerization behavior of AOMECE and ϵCL at different temperatures was the dependence of k_p^{app} on the temperature (Table 2 and Figure 1). The lactone monomer (i.e., ϵCL) follows the more logical trend where an increase in k_p^{app} was observed with increasing temperature. However, AOMECE exhibits a more “wavy” pattern (Table 2), which may be a proximity effect to the equilibrium monomer concentration of AOMECE. At -40 °C, the conversion of AOMECE as a function of time is linear up to a conversion of 95%, whereas at 30 °C the deviation from linearity occurs already at 80% conversion. This behavior is expected to become more prominent at higher temperatures

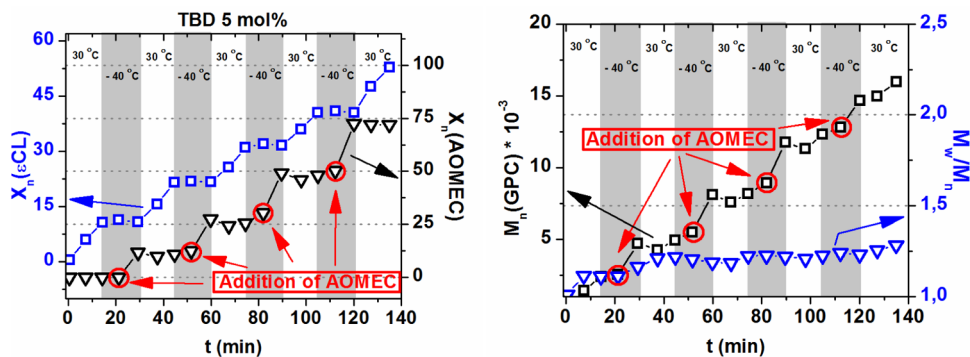


Figure 4. Repeating unit (X_n) of AOMECE and ϵ CL as a function of time (left); M_n and \bar{D} evolution (right), *in situ* variation in temperature between $T = -40$ °C and $T = 30$ °C during the copolymerization of AOMECE and ϵ CL.

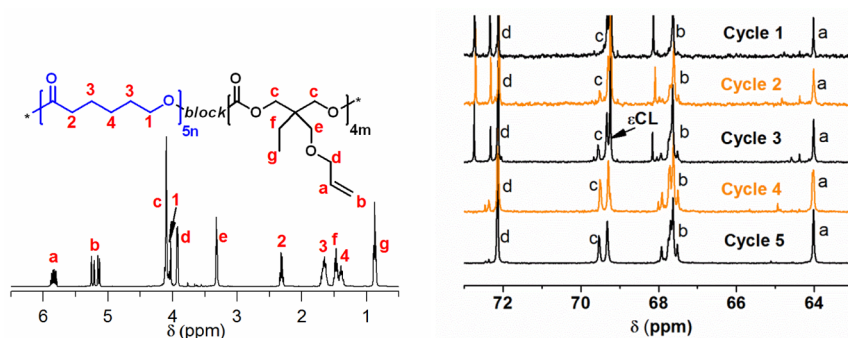


Figure 5. ^1H NMR of the copolymer obtained from *in situ*-polymerization with variation of temperature (left) block purity at the end of each cycle obtained from ^{13}C NMR analysis (right).

(i.e., 100 and 170 °C) (Figures 1 (bottom left) and (bottom right)) even though the trend is not obvious due to the high polymerization rates. In addition the difference in polymerization setup, i.e. solution at -40 and 30 °C versus bulk 100 and 170 °C could influence the rate of polymerization.

At all of the selected temperatures, the copolymerization of AOMECE and ϵ CL proceeded in a controlled manner with a linear increase in the molecular weight with conversion (Figure 2). However, at higher temperatures, an increase in dispersity was observed, which is similar to the results observed for polymerizations performed with $\text{Sn}(\text{Oct})_2/\text{ROH}$ as an initiating system.⁵⁴ The reason for these increased dispersity values remains unclear but it may be due to the higher rates of the transesterification reactions at higher temperature or the proximity to the ceiling temperature (T_c). On the basis of these studies, at lower temperatures, the difference in the polymerization rate is larger, and side reactions are absent. Therefore, “block-like” structures are obtained using our new synthetic approach.

The large difference in reactivity between AOMECE and ϵ CL at low temperatures can be used to prepare diblock copolymers by simultaneous addition of the two monomers (Table 2 and Figure 3). To emphasize this difference, the k_p^{app} ratio of these monomers was plotted as a function of temperature (Figure 5, left). At -40 °C, k_p^{app} (AOMECE) was as much as 400 times larger than k_p^{app} (ϵ CL). In contrast, at $T = 170$ °C, the k_p^{app} (AOMECE)/ k_p^{app} (AOMECE) ratio was only ~ 2 . The reason for this behavior may be the lower activation energy of 1,3-dioxan-2-ones compared to ϵ CL in TBD-catalyzed ring-opening polymerization. The different temperature dependences of the rate constants for the copolymerization of 2,2-dimethyl trimethylene carbonate and ϵ CL with Al based initiators have

been previously reported.^{53,55,56} The preference for one monomer over the other should translate to a more “block-like” structure of the copolymer. However, this may not be the case due to possible side reactions, especially transesterification reactions.

To gain insight into this issue, ^{13}C NMR spectroscopy was used to validate the microstructural features of the copolymer in relationship to the k_p^{app} ratio of the respective monomers at different temperatures (Figure 3, right).^{57,58} However, the chiral center of the ring-opened AOMECE monomer leads to a complicated ^{13}C NMR spectrum arising from the formation of different diastereomeric sequences (Scheme 2). By analyzing the $\text{CH}_2\text{-O}$ resonance signal of ϵ CL in different environments (i.e., monomer sequence ϵ CL- ϵ CL and the two sequences ϵ CL-AOMECE), the purity of the block copolymer was determined (Scheme 2 and Figure 3, right). At $T = -40$ °C, a single resonance line (a) was observed. As the temperature increased, an additional signal (A) appears, and the intensity of this signal increased as the temperature increased. Therefore, when the temperature increases, the concentration of ϵ CL-AOMECE sequences increases. The same is true for resonance lines c and d, where their intensity increases as the temperature increases. The microstructure of the copolymers of 2,2-dimethyl trimethylene carbonate and ϵ CL prepared with different types of initiators has been determined. However, in this case, no enantiomeric center was present. Therefore, all of the diads were assigned, and quantitative analysis was performed.⁵³

In summary, by changing the temperature from $+30$ to -40 °C, an on/off response toward ring-opening polymerization of ϵ CL was observed. In a mixture of AOMECE and ϵ CL, only AOMECE is converted at this temperature. To obtain a

multiblock copolymer, a solution of ϵ CL must be polymerized for a certain time at 30 °C and then cooled to -40 °C, and AOMECE should be added at this temperature followed by polymerization prior to heating to 30 °C again.

Multiblock Copolymer Synthesis by Polymerization of AOMECE and ϵ CL at $T = +30$ °C and $T = -40$ °C.

Variation in the temperature for the *in situ* polymerization of AOMECE and ϵ CL was used to prepare multiblock copolymers. The formation of a 9-block copolymer was performed in only 2.5 h (Figures 4 and 5). The TBD-catalyzed copolymerization of AOMECE and ϵ CL results in moderately high dispersity (approximately 1.5). However, the dispersity is strongly dependent on the conversion of ϵ CL (Figure 2, top right). Therefore, copolymers with lower dispersity can be prepared when the total conversion of ϵ CL remains low (Figure 4, right). This low conversion can be easily accomplished because the polymerization kinetics of ϵ CL compared to AOMECE exhibit an on/off response during the transition from $T = +30$ to $T = -40$ °C where AOMECE exhibits a high polymerization rate (Figure 4 and Table 2). The polymerization of ϵ CL was conducted in a 15 min window at 30 °C, enabling good control of the block length and dispersity. The reaction conditions were adjusted to obtain 10 repeating units for each P ϵ CL block and 15 repeating units for each PAOMECE block (Figure 4).

The block purity was determined at the end of each cycle, where one cycle consists of 30 min in which the temperature is changed from $T = +30$ to $T = -40$ °C and back to $T = +30$ °C. The high purity of the blocks was confirmed by the ¹³C NMR spectra obtained at the end of each cycle, and the ¹³C NMR spectra displayed only peaks associated with a pure block structure (Figure 5(right) and Scheme 2), which is clearly shown at the end of cycle 5 and represents the purified polymer. Therefore, no monomeric residues were present to obscure the spectra. The ¹H NMR spectrum obtained from the purified product revealed all of the resonance peaks corresponding to the two repeating units (Figure 5(left)). The theoretical calculated and experimentally determined monomeric ratios for the copolymers were in good agreement with each other (i.e., $(n_{\epsilon\text{CL}}/n_{\text{AOMECE}})_{\text{theoretical}} = 0.53$, $((n_{\epsilon\text{CL}}/n_{\text{AOMECE}})_{\text{experimental}} = 0.58)$, and the small discrepancy may originate from the purification of the AOMECE monomer. During the monomer synthesis prior to polymerization, opened oligomers may exist due to ring-closing depolymerization. Therefore, a consecutive end-capping reaction with acetic anhydride was performed prior to the additional distillation step. Although these end-capped oligomers are inert during polymerization, they will still affect the molar ratio of the added monomer in each cycle in the multiblock synthesis. In addition, an increase in the molecular weight was observed by GPC at each AOMECE addition cycle. In terms of dispersity, only a small increase was observed at a prolonged reaction time. The dispersity is consistent with what is commonly obtained in TBD-catalyzed ROP.⁵⁹

On the basis of these results, a new conceptual approach for the formation of multiblock copolymers via an *in situ* on/off kinetic response has been developed. Through careful evaluation of the kinetic behavior during copolymerization, the polymer architecture can be tailored where the length of each block can be predetermined based on the amount of AOMECE added at -40 °C and the length of temperature window for ϵ CL at 30 °C. We assume that this methodology is valid not only for the allyl functional carbonate monomer AOMECE but also for all six-membered ring carbonate

monomers that exhibit similar polymerization kinetics. In other words, macromolecular design via a kinetic on/off response of the monomers enables a straightforward approach for the preparation of multiblock polyester/polycarbonate copolymers.

CONCLUSIONS

The implementation of an *in situ* monomer-specific “on/off switch” for the ring-opening polymerization of functional carbonate monomers (i.e., AOMECE and ϵ CL) catalyzed by an organic catalyst (i.e., TBD) enabled the synthesis of a pure nine-block copolymer in only 2.5 h. The “on/off switch” was achieved via modulation of the temperature during polymerization from +30 to -40 °C. This transition resulted in a monomer-specific kinetic response (i.e., an on/off switch) for polymerization of ϵ CL and retardation of the AOMECE polymerization. This feature enabled the construction of a multiblock copolymer with a low dispersity ($D = 1.26$) and high control over the molecular weight and block length where each PAOMECE block was formed at $T = -40$ °C and each P ϵ CL block was formed at $T = 30$ °C.

The behavior was derived from the evaluation of the polymerization behavior of AOMECE and ϵ CL at different temperatures. This evaluation revealed an immense difference in the copolymerization kinetics at different temperatures that was connected to the purity of the blocks. The rate of polymerization is 400 times higher for AOMECE compared to ϵ CL at -40 °C, and at 100 °C, this rate was only 10 times higher. Thus, there is immense potential in every catalytic system that could be realized through careful investigation of that system's kinetic behavior.

ASSOCIATED CONTENT

Supporting Information

Data regarding the measurements of the k_p^{app} values from copolymerization of ϵ CL and AOMECE at different temperatures and GPC traces from copolymerization of AOMECE and ϵ CL with TBD and P2-*t*-Bu at 30 °C. This material is available free of charge via the Internet at <http://pubs.acs.org>.

AUTHOR INFORMATION

Corresponding Author

*(A.-C.A.) E-mail: aila@polymer.kth.se. Telephone: +46-8-790 82 74. Fax: +46-8-20 84 77.

Notes

The authors declare no competing financial interest.

ACKNOWLEDGMENTS

The authors acknowledge the ERC Advance Grant PARADIGM (Grant agreement no.: 246776) for their financial support of this work.

REFERENCES

- (1) Kamber, N. E.; Jeong, W.; Waymouth, R. M.; Pratt, R. C.; Lohmeijer, B. G. G.; Hedrick, J. L. *Chem. Rev.* **2007**, *107*, 5813.
- (2) Boyer, C.; Bulmus, V.; Davis, T. P.; Ladmiral, V.; Liu, J.; Perrier, S. *Chem. Rev.* **2009**, *109*, 5402.
- (3) Matyjaszewski, K. *Macromolecules* **2012**, *45*, 4015.
- (4) Zhang, N.; Samanta, S. R.; Rosen, B. M.; Percec, V. *Chem. Rev.* **2014**.
- (5) Zhang, Q.; Collins, J.; Anastasaki, A.; Wallis, R.; Mitchell, D. A.; Becer, C. R.; Haddleton, D. M. *Angew. Chem.* **2013**, *52*, 4435.

- (6) Gody, G.; Maschmeyer, T.; Zetterlund, P. B.; Perrier, S. *Nat. Commun.* **2013**, *4*, 2505.
- (7) Mespouille, L.; Coulembier, O.; Kawalec, M.; Dove, A. P.; Dubois, P. *Prog. Polym. Sci.* **2014**, *39*, 1144.
- (8) Albertsson, A. C.; Varma, I. K. *Biomacromolecules* **2003**, *4*, 1466.
- (9) Duda, A.; Kowalski, A.; Libiszowski, J.; Penczek, S. *Macromol. Symp.* **2005**, *224*, 71.
- (10) Duda, A.; Kubisa, P.; Lapienis, G.; Slomkowski, S. *Polimery* **2014**, *59*, 9.
- (11) Schindler, A.; Hibionada, Y. M.; Pitt, C. G. *J. Polym. Sci., Part A: Polym. Chem.* **1982**, *20*, 319.
- (12) Odelius, K.; Albertsson, A.-C. *J. Polym. Sci., Part A: Polym. Chem.* **2008**, *46*, 1249.
- (13) Tian, D.; Dubois, P.; Jerome, R.; Teyssie, P. *Macromolecules* **1994**, *27*, 4134.
- (14) Trollsås, M.; Löwnheim, P.; Lee, V.; Möller, M.; Miller, R.; Hedrick, J. L. *Macromolecules* **1999**, *32*, 9062.
- (15) Vanhoorne, P.; Dubois, P.; Jerome, R.; Teyssie, P. *Macromolecules* **1992**, *25*, 37.
- (16) Keul, H.; Schmidt, P.; Bernd, R.; Höcker, H. *Macromol. Symp.* **1995**, *253*, 243.
- (17) Mindemark, J.; Imholt, L.; Daniel, B. *Electrochim. Acta* **2015**, DOI: 10.1016/j.electacta.2015.01.074.
- (18) Bates, F. S.; Hillmyer, M.; Lodge, T. P.; Bates, C. M.; Delaney, K. T.; Fredrickson, G. H. *Science (80-)*. **2012**, *336*, 434.
- (19) Hillmyer, M. A.; Tolman, W. B. *Acc. Chem. Res.* **2014**, *47*, 2390.
- (20) Olsén, P.; Borke, T.; Odelius, K.; Albertsson, A.-C. *Biomacromolecules* **2013**, *14*, 2883.
- (21) Brannigan, R. P.; Walder, A.; Dove, A. P. *J. Polym. Sci., Part A: Polym. Chem.* **2014**, *52*, 2279.
- (22) Ryner, M.; Albertsson, A.-C. *Biomacromolecules* **2002**, *3*, 601.
- (23) Pospiech, D.; Komber, H.; Jehnichen, D.; Häussler, L.; Eckstein, K.; Scheibner, H.; Janke, A.; Kricheldorf, H. R.; Petermann, O. *Biomacromolecules* **2005**, *6*, 439.
- (24) Zhao, J.; Pahovnik, D.; Gnanou, Y.; Hadjichristidis, N. *Polym. Chem.* **2014**, *5*, 3750.
- (25) Martello, M. T.; Schneiderman, D. K.; Hillmyer, M. A. *ACS Sustain. Chem. Eng.* **2014**, *2*, 2519.
- (26) Nederberg, F.; Connor, E. F.; Möller, M.; Glauser, T.; Hedrick, J. L. *Angew. Chem.* **2001**, *42*, 2712.
- (27) Nederberg, F.; Connor, E.; Glauser, T.; Hedrick, J. *Chem. Commun.* **2001**, 2066.
- (28) Lohmeijer, B. G. G.; Pratt, R. C.; Leibfarth, F.; Logan, J. W.; Long, D. A.; Dove, A. P.; Nederberg, F.; Choi, J.; Wade, C.; Waymouth, R. M.; Hedrick, J. L. *Macromolecules* **2006**, *39*, 8574.
- (29) Zhang, L.; Nederberg, F.; Pratt, R. *Macromolecules* **2007**, 4154.
- (30) Kiesewetter, M.; Shin, E.; Hedrick, J. L.; Waymouth, R. M. *Macromolecules* **2010**, *43*, 2093.
- (31) Helou, M.; Miserque, O.; Brusson, J.-M.; Carpentier, J.-F.; Guillaume, S. M. *Chem.—Eur. J.* **2010**, *16*, 13805.
- (32) Makiguchi, K.; Ogasawara, Y.; Kikuchi, S.; Satoh, T.; Kakuchi, T. *Macromolecules* **2013**, *46*, 1772.
- (33) Delcroix, D.; Cuffin, A.; Susperregui, N.; Navarro, C.; Maron, L.; Martin-Vaca, B.; Bourissou, D. *Polym. Chem.* **2011**, *2*, 2249.
- (34) Couffin, A.; Delcroix, D.; Martin-Vaca, B.; Bourissou, D.; Navarro, C. *Macromolecules* **2013**, *46*, 4354.
- (35) Coady, D. J.; Horn, H. W.; Jones, G. O.; Sardon, H.; Engler, A. C.; Waymouth, R. M.; Rice, J. E.; Yang, Y. Y.; Hedrick, J. L. *ACS Macro Lett.* **2013**, *2*, 306.
- (36) Pratt, R. C.; Lohmeijer, B. G. G.; Long, D. a.; Waymouth, R. M.; Hedrick, J. L. *J. Am. Chem. Soc.* **2006**, *128*, 4556.
- (37) Olsson, J. V.; Hult, D.; Cai, Y.; Carcía-Gallego, S.; Malkoch, M. *Polym. Chem.* **2014**, *5*, 6651.
- (38) Zhao, J.; Pahovnik, D.; Gnanou, Y.; Hadjichristidis, N. *Macromolecules* **2014**, *47*, 3814.
- (39) Zhao, J.; Pahovnik, D.; Gnanou, Y.; Hadjichristidis, N. *J. Polym. Sci., Part A: Polym. Chem.* **2015**, *53*, 304.
- (40) Mathisen, T.; Albertsson, A.-C. *Macromolecules* **1989**, *22*, 3838.
- (41) Glavas, L.; Olsén, P.; Odelius, K.; Albertsson, A.-C. *Biomacromolecules* **2013**, *14*, 4150.
- (42) Olsén, P.; Undin, J.; Odelius, K.; Albertsson, A.-C. *Polym. Chem.* **2014**, *5*, 3847.
- (43) Sun, Y.; Olsén, P.; Waag, T.; Krueger, A.; Steinmüller-Nethl, D.; Albertsson, A.-C.; Finne-Wistrand, A. *Part. Part. Syst. Charact.* **2015**, *32*, 35.
- (44) Albertsson, A.-C.; Ljungquist, O. *J. Macromol. Sci.—J. Appl. Polym. Chem.* **1986**, *A23*, 393.
- (45) Arias, V.; Höglund, A.; Odelius, K.; Albertsson, A.-C. *Biomacromolecules* **2014**, *15*, 391.
- (46) Undin, J.; Finne-Wistrand, A.; Albertsson, A.-C. *Biomacromolecules* **2014**, *15*, 2800.
- (47) Olsén, P.; Odelius, K.; Albertsson, A.-C. *Macromolecules* **2014**, *47*, 6189.
- (48) Albertsson, A.-C.; Eklund, M. *J. Polym. Sci., Part A Polym. Chem.* **1994**, *32*, 265.
- (49) Albertsson, A.; Sjöling, M. *J. Macromol. Sci.—J. Appl. Polym. Chem.* **1992**, *A29*, 43.
- (50) Kühling, S.; Keul, H.; Höcker, H. *Macromol. Chem. Phys.* **1990**, *191*, 1611.
- (51) Kühling, S.; Keul, H.; Hocker, H. *Macromol. Chem. Phys.* **1992**, *193*, 1207.
- (52) Schlaad, H.; Kukula, H.; Rudloff, J.; Below, I. *Macromolecules* **2001**, *34*, 4302.
- (53) Keul, H.; Höcker, H.; Leitz, E. *Macromol. Chem. Phys.* **1988**, *189*, 2303.
- (54) Dubois, P.; Ropson, N.; Jérôme, R.; Teyssié, P. *Macromolecules* **1996**, *29*, 1965.
- (55) Duda, A.; Penczek, S. *Macromol. Chem., Macromol. Symp.* **1991**, *42/43*, 135.
- (56) Wurm, B.; Keul, H.; Höcker, H. *Macromol. Chem. Phys.* **1994**, *195*, 3489.
- (57) Guerin, W.; Helou, M.; Slawinski, M.; Brusson, J.-M.; Guillaume, S. M.; Carpentier, J.-F. *Polym. Chem.* **2013**, *4*, 3686.
- (58) Aguirre-Chagala, Y.; Santos, L. J.; Herrera-Nájera, R.; Herrera-Alonso, M. *Macromolecules* **2013**, *46*, 5871.
- (59) Nederberg, F.; Lohmeijer, B. G. G.; Leibfarth, F.; Pratt, R. C.; Choi, J.; Dove, A. P.; Waymouth, R. M.; Hedrick, J. L. *Biomacromolecules* **2007**, *8*, 153.